Polymers for Advanced Technologies

WILEY

polymers for advanced technologies

RESEARCH ARTICLE OPEN ACCESS

Reduced Shear Degradation of Poly(Lactic Acid) in Hybrid Composites Containing Carbon Nanotubes and Carbon Microfibers

Roland Petrény[1] | Kristof Molnar[2,3] | Judit E. Puskas[2] | László Mészáros[1,4]

[1]Faculty of Mechanical Engineering, Department of Polymer Engineering, Budapest University of Technology and Economics, Budapest, Hungary | [2]Department of Food, Agricultural and Biological Engineering, College of Food, Agricultural and Environmental Science, The Ohio State University, Wooster, Ohio, USA | [3]Department of Biophysics and Radiation Biology, Laboratory of Nanochemistry, Semmelweis University, Budapest, Hungary | [4]HUN-REN-BME Research Group for Composite Science and Technology, Budapest University of Technology and Economics, Budapest, Hungary

Correspondence: László Mészáros (meszaros.laszlo@gpk.bme.hu)

Received: 16 May 2025 | **Revised:** 26 July 2025 | **Accepted:** 4 August 2025

Funding: This work was supported by the European Union's Horizon 2020 research and innovation program under Marie Skłodowska-Curie grant agreement no. 872152 (GREEN MAP). Project no. TKP-6-6/PALY-2021 has been implemented with the support provided by the Ministry of Culture and Innovation of Hungary from the National Research, Development and Innovation Fund, financed under the TKP2021-NVA funding scheme. The authors acknowledge the Ministry of Culture and Innovation of Hungary for support from the National Research, Development and Innovation Fund through grant no. NKKP ADVANCED 149578. The authors would like to acknowledge USDA-NIFA-Hatch project 7003189.

Keywords: carbon fibre | hybrid | linear viscoelasticity | nano-structure | rheological properties

ABSTRACT

In this study, we investigated carbon nanotube reinforced nanocomposites and hybrid composites containing both carbon microfibers and carbon nanotubes of poly(lactic acid) (PLA) and the effect of the fillers on the molecular weight of the PLA matrix. Dynamic mechanical analysis and rheometric measurements revealed that incorporating either carbon nanotubes or carbon microfibers into pure PLA reduces the linear viscoelastic (LVE) range. This reduction arises from early disruption of interfacial bonds between the matrix and the reinforcements, as well as the breakdown of contacts among aggregated nanotubes under small strains, both of which trigger nonlinearity. In contrast, adding carbon nanotubes to carbon microfiber-reinforced PLA to form a hybrid composite shifted the LVE limit to higher strain values. This improvement is attributed to the nanotubes effectively bridging the matrix–fiber interfaces, enhancing interfacial stress transfer and delaying the onset of microstructural rearrangements responsible for nonlinear behavior. Size Exclusion Chromatography (SEC) showed that the molecular weight of the matrix decreased significantly in the composites containing only carbon microfibers, while the presence of the carbon nanotubes prevented the molecular chains from weight reduction. This supported the hypothesis that the molecular chains and the well-dispersed carbon nanotubes form an entangled network, which is a much more stable system that can protect from chain breakage during processing.

Abbreviations: CF, Carbon fiber; CNT, Carbon nanotube; DMA, Dynamic mechanical analysis; LVE, Linear viscoelastic; MFI, melt flow index; PLA, Poly(lactic acid); SEC, Size exclusion chromatography; SEM, Scanning electron microscopy; THF, Tetrahydrofuran.

1 | Introduction

In recent years, composites reinforced with nanoscale fillers—particularly carbon nanotubes (CNTs)—and hybrid composites combining both nano- and microscale fillers have attracted considerable attention. Carbon microfibers and CNTs are widely used not only for their outstanding mechanical properties but also for their excellent thermal and electrical conductivity. In hybrid systems, microfibers typically serve as the primary load-bearing components, while nanoparticles facilitate stress transfer between the polymer matrix and the reinforcement. However, the mechanisms governing this stress transfer remain only partially understood, limiting the ability to optimize composite performance [1–6].

Simultaneously, there is a growing demand for sustainable materials in structural and functional applications. Recent reviews highlight the shift toward eco-friendly biocomposites—made from natural fibers such as flax, hemp, jute, cork, or silk combined with biodegradable matrices—as a key step toward achieving the UN Sustainable Development Goals. These materials offer benefits such as compostability, recyclability, and a lower environmental impact, while still delivering competitive mechanical strength and thermal stability. Despite challenges in fiber–matrix compatibility and processing consistency, their appeal lies in the balance between performance and sustainability [7–10]. Among bioplastics, poly(lactic acid) (PLA) is especially attractive due to its compostability, biocompatibility, and processability. However, understanding the viscoelastic behavior of PLA-based composites is essential—particularly within the linear viscoelastic (LVE) range, where stress and strain remain proportional, and commonly applied mechanical models are valid [11–14]. This range is bounded by the onset of irreversible structural transformations, such as chain orientation, crystalline realignment, or interfacial debonding, which can be especially pronounced in PLA due to its susceptibility to molecular weight reduction under shear [15–19].

In composite materials, the LVE range is typically defined as the strain (or stress) amplitude over which the storage modulus and loss modulus remain constant. Exceeding this window leads to microstructural changes such as fiber–matrix debonding, filler network breakdown, or polymer chain slippage, which result in non-linear viscoelastic responses. As composite stiffness increases—through the addition of rigid fillers or higher volume fractions—the LVE range tends to narrow. This occurs because stiff inclusions restrict chain mobility, generate local stress concentrations, and elevate interfacial stresses that promote debonding; the critical strain at which the storage modulus starts to decrease shifts to lower values. These constraints present design trade-offs: while stiffness enhances strength, it limits its usable deformation ranges. Extending the LVE range in stiff systems often requires strategies such as surface-modified fillers, soft secondary phases, or hierarchical filler architectures to better distribute stress and maintain interface integrity [20–22].

In nanocomposites, non-linearity is often attributed to the disruption of loosely bound 3D CNT networks or the breaking of weak interactions between CNTs and polymer chains. In hybrid systems, the interaction mechanisms become more complex. An additional factor is shear-induced molecular weight degradation, which can significantly influence the LVE threshold by altering the chain length and entanglement density of the matrix [23–25]. Interestingly, previous studies have shown that the formation of an interphase—where polymer chain motion is restricted by proximity to filler surfaces—may delay interface failure and even protect chains from degradation under strain, thereby shifting the onset of non-linear behavior [3, 26].

While previous research has addressed filler-induced changes in rheological performance, little is known about how hybrid reinforcement architectures affect the onset of non-linear viscoelasticity and processing-related molecular weight degradation. Therefore, the aim of our research is to explore how the combination of carbon microfibers and carbon nanotubes influences the linear viscoelastic behavior and molecular stability of poly(-lactic acid) (PLA)-based composites.

2 | Materials and Methods

The compositions of the materials investigated are shown in Table 1.

The polymer matrix Ingeo 4043D (NatureWorks LLC, USA) PLA has a tensile strength of 53 MPa, a tensile modulus of 3.6 GPa, an elongation at break of 6%, a density of 1.24 g/cm^3 and a melt flow index (MFI) (2.16 kg/210°C) of 6 g/10 min based on the material data sheet. The D-lactide content of the PLA was 4.8% [27].

Nanocyl NC7000 (Nanocyl SA, Belgium) multi-walled carbon nanotubes produced by catalytic chemical vapor deposition with an average diameter of 9.5 nm, an average length of 1.5 µm, carbon content of 90 wt%, less than 1 wt% of transition metal oxide content, and specific surface area between 250 and 300 m^2/g were used.

PANEX PX35 (Zoltek Zrt., Hungary) chopped carbon microfibers with a tensile strength of 3,800 MPa, a tensile modulus of 242 GPa, an elongation at break of 1.5%, a density of 1.81 g/cm^3, a fiber diameter of approximately 7.2 µm, and a carbon content of 95% were used as micron-size reinforcement. The initial fiber length was 6 mm, and the fibers had silane sizing for polar matrices.

Before compounding, the PLA was dried in a Faithful WGLL-125 BE (Huanghua Faithful Instrument Co. LTD, China) drying oven for 4 h at 80°C according to the recommendation of the manufacturer. First, the reinforcing materials were mixed with the PLA pellets in a plastic box; then the materials were compounded with a Labtech Engineering Co. Ltd. LTE 26–44 twin-screw extruder (Labtech Engineering Co. Ltd., Thailand) with a screw speed of 25.1/min and zone temperatures of 180°C, 190°C, 190°C, 190°C, 190°C, 200°C, 200°C, 200°C, 200°C, and 200°C and die temperature of 190°C. Pellets were prepared from the filaments with a Labtech LZ-120/VS (Labtech Engineering Co. Ltd., Thailand) pelletizer. Before injection molding, the granules were dried again at 80°C for 4 h.

1A type dumbbell tensile specimens (EN ISO 527-2:2019) were produced by an Arburg Allrounder Advance 270S 400–170

TABLE 1 | Composition of the materials investigated.

CNT [wt%]	0	0.25	0.5	0.75	1.00	0	0.25	0.5	0.75	1.00
CF [wt%]	0	0	0	0	0	30	30	30	30	30
Designation	PLA	PLA + 025CNT	PLA + 05CNT	PLA + 075CNT	PLA + 1CNT	PLA + 30CF	PLA + 30CF + 025CNT	PLA + 30CF + 05CNT	PLA + 30CF + 075CNT	PLA + 30CF + 1CNT

(Arburg GmbH, Germany) injection molding machine, with a melt temperature of 200°C, a mold temperature of 25°C, and an injection pressure of 1200 bar.

Tetrahydrofuran (THF, Fisher Chemical T3974) was used to prepare samples for Scanning Electron Microscopy (SEM) analysis, which contained about 0.025% butylated hydroxytoluene as a preservative, had a molecular weight of 72.11 g/mol, and a density of 0.88 g/cm^3. 1–2 mg/mL solutions were prepared in THF, and the samples were let to dissolve on a shaker (IKA MS3 digital) until complete dissolution. Then, 1 mL of this solution was filtered using a 0.45 μm poly(tetrafluor ethylene) syringe filter (diameter 13 mm, WVR 514–0069). Syringe filters were washed by pushing through 1 + 1 mL pure THF. Then, they were left under the hood to dry, then dried further until constant weight under vacuum at room temperature. The filters then were cut open and used for SEM analysis.

Size exclusion chromatography (SEC) measurements were performed using a system consisting of an Agilent 1260 infinity isocratic pump, a Wyatt Eclipse DUALTEC separation system, an Agilent 1260 infinity variable wavelength detector (UV), a Wyatt OPTILAB T-rEX interferometric refractometer (dRI), a Wyatt DAWN HELOS-II multi-angle static light scattering detector (MALS) with a built-in dynamic light scattering (DLS) module, a Wyatt ViscoStar-II viscometer, an Agilent 1260 infinity standard autosampler, and 6 StyragelVR columns (HR6, HR5, HR4, HR3, HR1, and H0.5). The columns were thermostated at 35°C and THF, continuously distilled from CaH_2, was used as the mobile phase at a flow rate of 1 mL/min. The results were analyzed using the ASTRA 7 software (Wyatt Technology). Absolute molecular weights were obtained using a dn/dc of 0.042 mL/g for PLA. Samples were first dissolved in THF from the distillation; then 1 mL was filtered into the SEC vials using a 0.45 μm PTFE syringe filter. In every case, 100 μL was injected. A polystyrene standard with $M_n = 30$ kg/mol, Đ 1.05, (Pressure Chemical, Pittsburgh, PA) was used for quality control only.

A DMA Q800 dynamic mechanical analyzer (DMA, TA Instruments, USA) was used in a 3-point clamped bending arrangement with a support distance of 35 mm. 10 × 4 × 60 mm samples were machined out from the injection molded specimens. The limit of LVE was determined by stretch-sweep type measurements, where the loss factor was tested as a function of amplitude. Ten points per decade on a logarithmic scale of amplitude, from 0.1 μm to 1,000 μm, were measured. In all cases, the test was carried out at room temperature (25°C), below the glass transition temperature (T_g) of the materials, with a heat holding time of 5 min and a sinusoidal excitation frequency of 1 Hz. The LVE limit was defined at the amplitude where the value of the loss factor deviated by 10% from the plateau value [14]. Triplicate measurements per material were performed.

Amplitude sweep tests were performed with a constant 6.28 rad/s angular frequency on a TA Instruments Discovery Hybrid HR20 rheometer. The samples were molded onto the 25 mm diameter parallel plate at 180°C for the measurements. The range of the oscillation strain sweep was between 0.005 and 500%, and the gap size was 250 μm.

To examine the fracture surfaces, the injection molded dumbbell specimens were tensile tested using a Zwick Z20 tensile testing machine at a test speed of 2 mm/min.

The electron microscopy images of the solution filters and the fracture surface of the tensile tested specimens were taken with a JEOL JSM 6380LA scanning electron microscope, after sputtering with gold.

3 | Results and Discussion

3.1 | Dynamic Mechanical Analysis

The purpose of the dynamic mechanical analysis in this study was to investigate how the presence of carbon nanotubes, carbon microfibers, and their combination influences the limit of linear viscoelastic behavior in PLA-based composites. Special attention was given to whether the addition of nanotubes could help maintain or even extend the LVE range, which typically becomes narrower when reinforcing additives are introduced. The LVE range was determined by plotting the loss factor as a function of increasing amplitude using strain sweep measurements at constant frequency (Figure 1a). The point where the function deviates by more than 10% from the constant (plateau) value indicates a deviation from LVE behavior. The highest amplitude was observed in the case of pure PLA. The amplitude goes through a minimum with increasing carbon nanotube (CNT) content. This is typically explained in the literature by the aggregation of the CNT particles that irreversibly break up even under relatively small deformation [15, 16]. In a strain-sweep type measurement, the CNT particles slip on each other even at small deformations, causing irreversible structural changes that cause a deviation from the LVE behavior. However, the plateau modulus remains unchanged with increasing CNT content.

In the case of the composite with 30 wt% carbon microfiber (CF), the amplitude at the LVE limit drops precipitously and then increases with the addition of CNT. The plateau modulus increases almost six-fold relative to pure PLA but remains relatively unchanged with increasing CNT content. However, compared with PLA containing only CF, the addition of CNT shifted the limit of LVE behavior towards higher amplitudes. This can be explained by that generally, in the case of composites containing micron-sized reinforcing materials, high filler content can cause the reinforcing materials to contact each other, and this contact is broken even at small deformations, pushing the LVE limit of the material lower compared with the pure matrix material. However, the lowering of the LVE limit compared with the pure matrix material has been shown in many studies, even at very low filler contents, when the contact between the reinforcing materials is not yet significant. This can be explained by the fact that the reinforcing materials start to orient towards the load or the fiber-matrix bond breaks. In composites, since the modulus, and hence the deformability, of the fiber and the matrix differ significantly, this latter mechanism is dominant. However, compared with PLA containing only CF, the addition of CNT shifted the limit of LVE behavior towards higher amplitudes. One reason is that in the case of the PLA matrix, the CNTs are uniformly distributed so that the interaction between nanoparticles described for nanocomposites is less significant. In the hybrid composites, according to previous studies, the rigid amorphous interphase is also formed in the vicinity of the carbon fibres and the uniformly distributed carbon nanotubes, and the interphases of the different reinforcing materials overlap [3, 26]. Therefore, the modulus increases gradually from the matrix towards the fibre, so that the rupture between the different modulus parts under load occurs at higher loads [28]. Another explanation could be that the uniformly distributed nanotubes increase the shear in the melt so much that the molecular weight starts to decrease, thereby slightly increasing the LVE limit. However, the role of molecular weight on the LVE range is presumably smaller than the effect of the microstructure.

4 | Rheology

Rotational rheometry was applied to complement the DMA results and to provide insights into the viscoelastic behavior of the composites under melt-state conditions, which are more representative of polymer processing. The results showed that the addition of CNT to the pure PLA significantly decreases the limit of the LVE range (Figure 2). The addition of the CF to the PLA reduces more significantly the limit of the LVE behavior, which

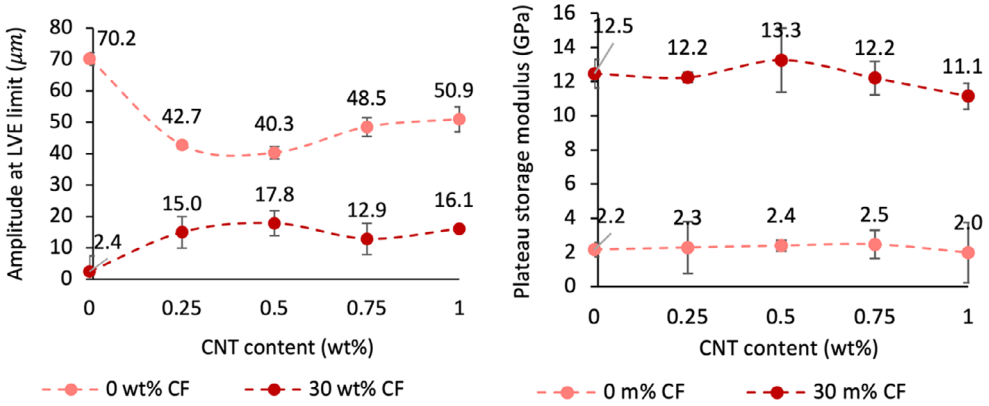

FIGURE 1 | (a) linear viscoelastic range of the PLA matrix nano- and hybrid composites (b) plateau storage modulus as a function of nanotube content.

can be explained by the fact that the interface between the fibers and the matrix breaks up at a relatively low strain. However, in the hybrid composites, the addition of the CNT does not cause a significant reduction in the LVE range. Moreover, by adding 0.25 wt% CNT to the CF-reinforced composite, the LVE range increases compared with the composite containing only CF. This can be explained by the fact that the CNTs in aggregated form contact with each other over a large surface area, and this loose contact breaks up easily at low strain. In hybrid composites, the molecular chains of the matrix are bonded to the CFs and entangled around the CNTs; this results in overlapping interphases around the reinforcing materials. This causes a more gradual stress transfer between the matrix and the reinforcing materials induced by the strain excitation so that the interfaces separate irreversibly at higher deformation.

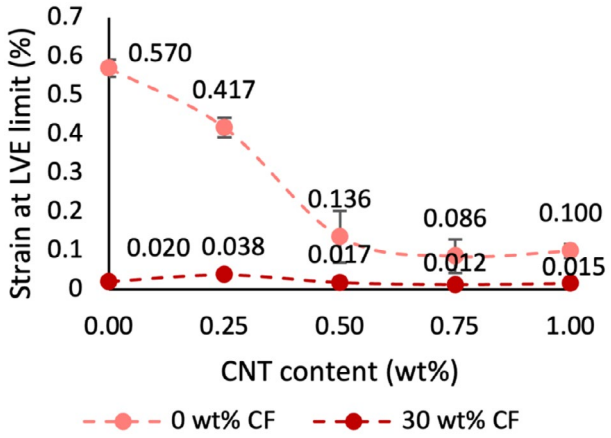

FIGURE 2 | Linear viscoelastic range measured by rheometer of the PLA matrix nano- and hybrid composites.

5 | Size Exclusion Chromatography

Size exclusion chromatography was applied to examine the molecular weight distribution of the PLA matrix after processing. The goal was to identify degradation effects induced by melt processing and to separate these from the property changes caused by the presence of carbon microfibers and carbon nanotubes. By doing so, we aimed to clarify the specific role of each type of reinforcement, independent of shear-induced molecular degradation. SEC chromatograms of the PLA separated from the PLA + CNT samples by simple filtration can be seen in Figure 3 and data are collected in Table 2. There is no difference between the chromatograms of the pure PLA and the PLA separated from the nanocomposites; thus, the addition of CNT did not change the molecular weight of the PLA (Figure 3a). This can be explained by two factors. On the one hand, the CNTs are partially in an aggregated form in the nanocomposites; thus, they cannot increase the shear during the processing. On the other hand, the dispersed, individual nanoparticles are well embedded in the matrix and can move with the molecules.

By adding CFs to the PLA, the average molecular weight decreases significantly compared with the pure PLA (Figure 3b and Table 2). This can be explained by the greatly increased shear in the melt during the extrusion and injection molding, which results in the breaking of the molecular chains. However, by adding 0.5 wt% CNT to the microfiber reinforced

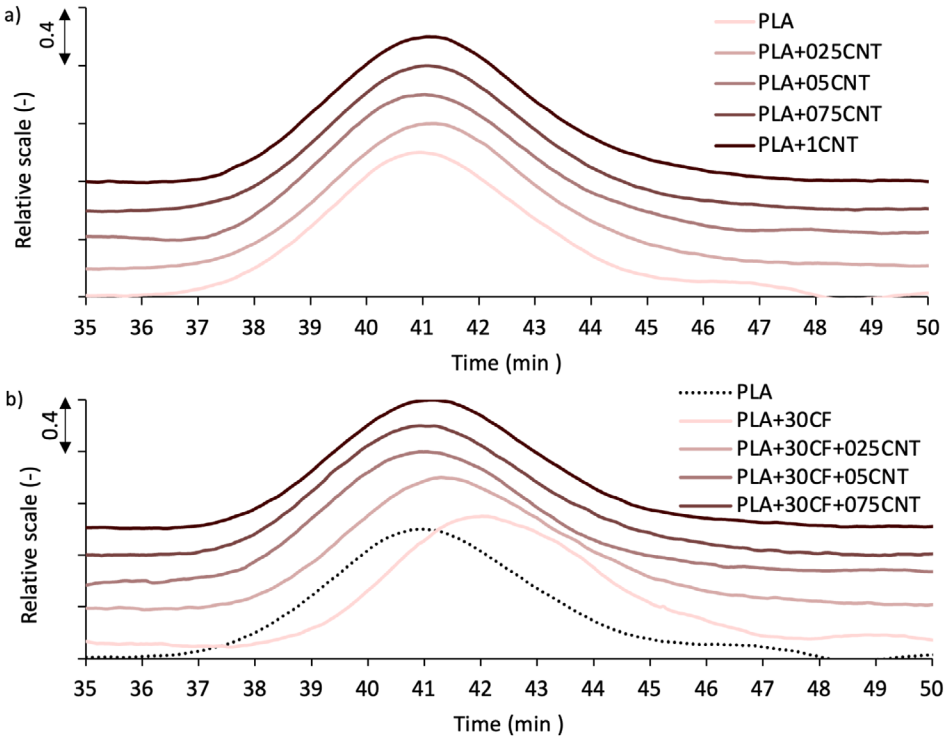

FIGURE 3 | (a) Size-exclusion chromatograms of the pure PLA and the nanocomposites, (b) of the pure PLA, the only carbon fiber reinforced, and the hybrid composites.

composite, the average molecular weight remained unchanged compared with the pure PLA's. The explanation for this can be that the molecular chains are entangled around the CNTs, and this can protect the molecules from breaking. In a hybrid composite, in which the CNTs are well-dispersed, not only are the molecules and the nanotubes entangled around each other, but also the nanotubes themselves entangle around each other, creating a much more stable network.

TABLE 2 | SEC data of the samples.

Sample name	M_w (kg/mol)	M_n (kg/mol)	$Đ$ (–)
PLA	125.1	78.6	1.59
PLA + 0.25CNT	122.9	81.0	1.52
PLA + 0.5CNT	126.3	80.3	1.57
PLA + 0.75CNT	129.7	87.7	1.48
PLA + 1CNT	126.4	75.7	1.67
PLA + 30CF	82.0	57.6	1.42
PLA + 30CF + 0.25CNT	103.2	65.6	1.57
PLA + 30CF + 0.5CNT	113.8	64.6	1.76
PLA + 30CF + 0.75CNT	121.9	84.3	1.45
PLA + 30CF + 1CNT	118.6	78.9	1.50

Note: Mn-number average molecular mass, Mw-weight average molecular mass, Đ-dispersity index.

6 | Scanning Electron Microscopy

We prepared SEM micrographs of the material residues on the SEC filters to further investigate the matrix reinforcement relationships. (Figure 4a). shows that the CNTs form an intertwined network, which indicates that, despite the filter pores being 0.45 μm in size, the nanoparticles can be filtered out of the composite solution. (Figure 4b–d) shows significant matrix residue on CNTs and CFs after filtration, indicating strong interactions between the nanoparticles and the matrix, and localized fiber–matrix bonding through the nanotube coils. This confirms the presence of a rigid amorphous interphase with restricted mobility around the fillers and that the molecular chains coil up on the nanotubes, which may play a role in the fact that in the presence of nanotubes, the molecular chains do not degrade during processing. (Figure 4c,d) show that in the hybrid composites, these interphases around the micro-and nanofibers overlap each other, which may result in an enhanced stress transfer from the matrix to the fibers. However, the absence of polymer attachment on the fibers in regions where there are no CNTs and the reduced linear viscoelastic limit suggest that the fiber–matrix interaction is much weaker in the carbon fiber-only composite.

To confirm the better dispersion of nanoparticles in the hybrid composites, SEM images were also taken of the fracture

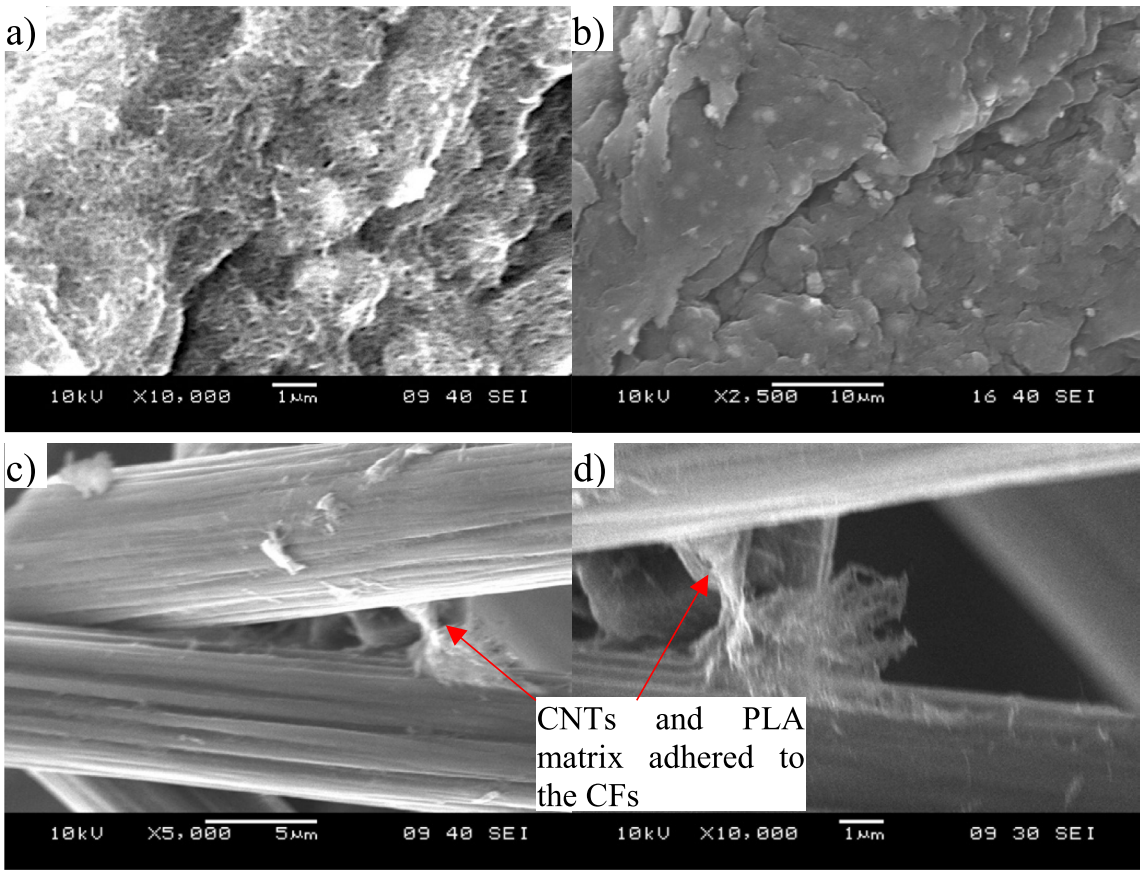

FIGURE 4 | Scanning electron microscope micrographs (a, b) of the PLA + 05CNT, (c, d) of the PLA + 30CF + 05CNT composites on the SEC filter.

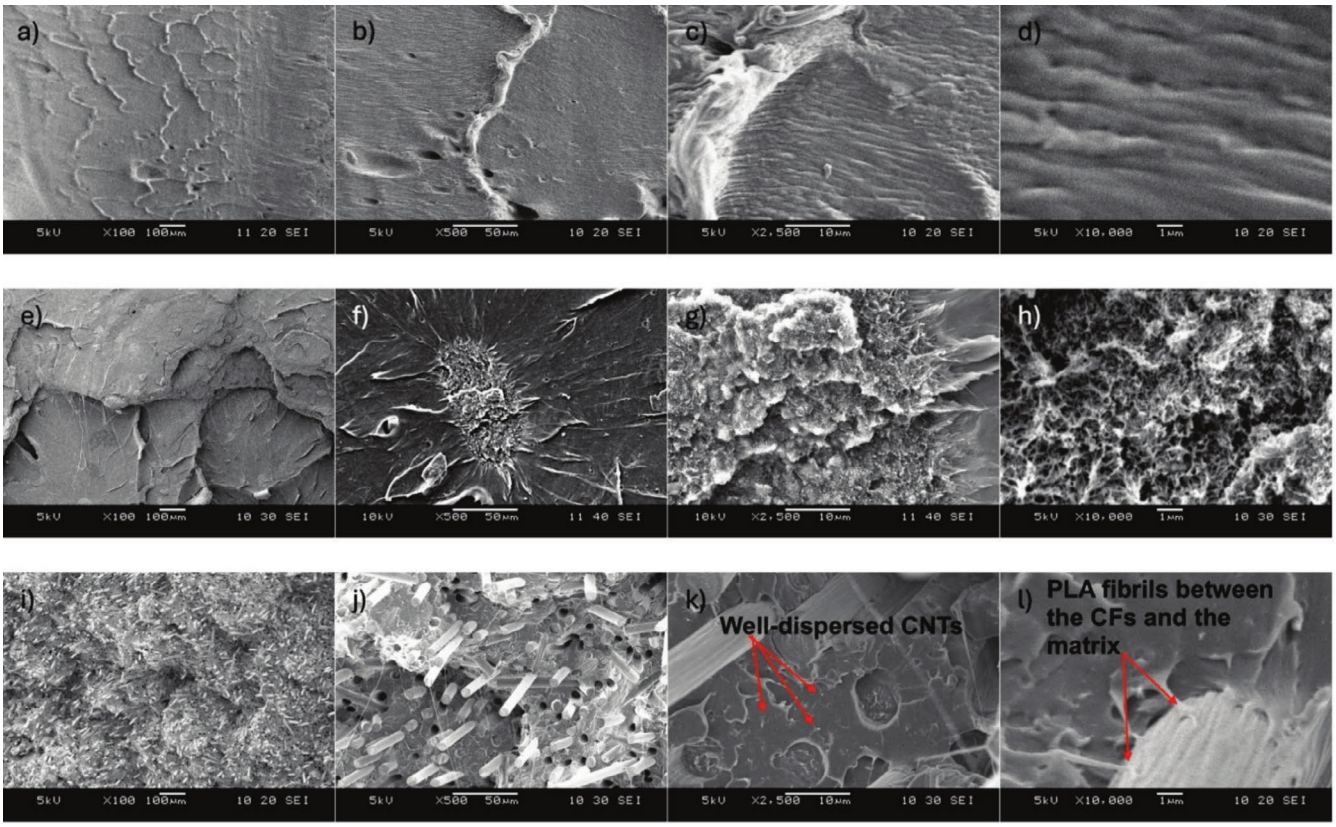

FIGURE 5 | Scanning electron microscope micrographs of the fracture surface of (a–d): pure, unfilled PLA, (e–h): PLA containing 0.5 wt% CNT, (i–l): PLA containing 30 wt % CF and 0.5% CNT.

surface of the injection molded and then tensile tested specimens. In the unfilled PLA reference (Figure 5a–d), fracture surfaces exhibited characteristic smooth, planar facets indicative of brittle failure and limited energy dissipation. Upon incorporation of 0.5 wt % CNT, low-magnification SEM images (Figure 5e,f) revealed island-like CNT bundle inclusions, suggesting the presence of micron-scale aggregates, which acted as the starting point of the failure. High-magnification micrographs (Figure 5g,h) showed that these aggregates consist of poorly dispersed CNTs, which are only partially impregnated by the matrix material, which may also be the reason for the decreasing linear viscoelastic range. In the hybrid PLA composite containing 30 wt % carbon fiber and 0.5 wt % CNT, SEM observations demonstrated preferential localization of CNTs at the fiber–matrix interface. Numerous nanoscale fibrils were observed to emanate from fiber surfaces into the PLA matrix, indicating effective CNT wetting during melt compounding. This interfacial enrichment reinforces the interphase region, and thus, a fraction of the applied stress is transferred into the carbon fibers via the carbon nanotubes. Because the reinforcing materials have a very high modulus, they deform less under the shear stress, thus protecting the polymer chains intertwined with them from the full amplitude of the shear strain.

7 | Conclusions

This research of PLA-based systems—ranging from carbon nanotube (CNT) nanocomposites to carbon microfiber (CF) and CNT hybrid composites—has revealed clear trends in viscoelastic and molecular behavior. Both dynamic mechanical analysis and rheometric testing confirmed that the incorporation of either CNTs or CFs into neat PLA reduces the linear viscoelastic (LVE) window, as interfacial bonds and filler–filler contacts begin to fail under very small strains, triggering an early transition to non-linear response. The hybrid architecture—where CNTs are introduced into a CF-reinforced matrix—reverses this trend. Here, overlapping interphase regions around each filler create a more gradual, strain-dependent stress transfer pathway. As a result, the composite retains its LVE behavior to substantially higher strains before irreversible interfacial debonding occurs. Size-exclusion chromatography of PLA extracted from each composite showed a related molecular phenomenon: CF-only systems suffer marked molecular weight loss due to shear-induced chain scission, whereas the CNT/CF hybrids exhibit minimal degradation. This supports the hypothesis that CNTs establish an entangled network with PLA chains that stabilizes the polymer against processing stresses and inhibits chain breakage. Together, these findings suggest that in bio-based hybrid composites the nanoscale fillers not only reinforce mechanical performance but also protect molecular integrity—thereby extending the lifecycle of the bioplastics. In the future, tailoring CNT surface chemistry could further optimize interphase thickness and stress transfer, potentially broadening the LVE regime even in high-stiffness formulations. Moreover, systematic variation of filler aspect ratio and volume fraction would clarify the interplay between interfacial area and chain entanglement density. Applying this hybrid approach to other

bioplastics could generalize the strategy across biodegradable matrices.

Acknowledgments

Project no. TKP-6-6/PALY-2021 has been implemented with the support provided by the Ministry of Culture and Innovation of Hungary from the National Research, Development and Innovation Fund, financed under the TKP2021-NVA funding scheme. The authors acknowledge the Ministry of Culture and Innovation of Hungary for support from the National Research, Development and Innovation Fund through grant no. NKKP ADVANCED 149578. The authors would like to acknowledge USDA-NIFA-Hatch project 7003189. The authors acknowledge funding from the European Union's Horizon 2020 research and innovation program under Marie Skłodowska-Curie grant agreement no. 872152 (GREEN MAP).

Conflicts of Interest

The authors declare no conflicts of interest.

Data Availability Statement

The data that support the findings of this study are available on request from the corresponding author. The data are not publicly available due to privacy or ethical restrictions.

References

1. T. Siriwas, S. Pichaiyut, M. Susoff, S. Petersen, and C. Nakason, "Graphene-Filled Natural Rubber Nanocomposites: Influence of the Composition on Curing, Morphological, Mechanical, and Electrical Properties," *Express Polymer Letters* 17 (2023): 819–836, https://doi.org/10.3144/expresspolymlett.2023.61.

2. S. S. Godara and P. K. Mahato, "Potential Applications of Hybrid Nanocomposites," *Materials Today: Proceedings* 18 (2019): 5327–5331, https://doi.org/10.1016/j.matpr.2019.07.557.

3. L. Mészáros, A. Horváth, L. M. Vas, and R. Petrény, "Investigation of the Correlations Between the Microstructure and the Tensile Properties Multi-Scale Composites With a Polylactic Acid Matrix, Reinforced With Carbon Nanotubes and Carbon Fibers, With the Use of the Fiber Bundle Cell Theory," *Composites Science and Technology* 242 (2023): 110154, https://doi.org/10.1016/j.compscitech.2023.110154.

4. T. T. Koilraj and K. Kalaichelvan, "Hybrid Nanocomposites—A Review," *Applied Mechanics and Materials* 766-767 (2015): 50–56, https://doi.org/10.4028/www.scientific.net/AMM.766-767.50.

5. S. Siengchin, "A Review on Lightweight Materials for Defence Applications: Present and Future Developments," *Defence Technology* 24 (2023): 1–17, https://doi.org/10.1016/j.dt.2023.02.025.

6. P. Csvila and T. Czigány, "Multifunctional Energy Storage Polymer Composites: The Role of Nanoparticles in the Performance of Structural Supercapacitors," *Express Polymer Letters* 18 (2024): 1023–1038, https://doi.org/10.3144/expresspolymlett.2024.78.

7. S. Palaniappan, M. Singh, M. R. Sanjay, and S. Siengchin, "Eco-Friendly Biocomposites: A Step Towards Achieving Sustainable Development Goals," *Applied Science and Engineering Progress* 17 (2024): 7373–7375, https://doi.org/10.14416/j.asep.2024.02.003.

8. S. Ullah, Z. Akhter, A. Palevicius, and G. Janusas, "Review: Natural Fiber-Based Biocomposites for Potential Advanced Automotive Applications," *Journal of Engineered Fibers and Fabrics* 20 (2025): 11468, https://doi.org/10.1177/15589250241311468.

9. A. Khan, S. M. Sapuan, E. S. Zainudin, and M. Y. M. Zuhri, "Physical, Mechanical and Thermal Properties of Novel Bamboo/Kenaf Fiber-Reinforced Polylactic Acid (Pla) Hybrid Composites," *Composites Communications* 51 (2024): 102103, https://doi.org/10.1016/j.coco.2024.102103.

10. M. Musioł, J. Rydz, W. Sikorska, H. Janeczek, and S. Jurczyk, "Organic Recycling Challenges of (Bio)Degradable Packages: Degradation Studies of Polylactide/Cork Composites," *Express Polymer Letters* 18 (2024): 868–880, https://doi.org/10.3144/expresspolymlett.2024.64.

11. J. Gomez-Caturla, D. Lascano, N. Montanes, et al., "Manufacturing and Characterization of Highly Environmentally-Friendly Composites With Polylactide Matrix and Mango Kernel Seed Flour," *Express Polymer Letters* 17 (2023): 334–351, https://doi.org/10.3144/expresspolymlett.2023.24.

12. G. Szabó and K. Váradi, "FE Micromodel of a Cord-Rubber Composite Test Specimen Subjected to Uniaxial Tension," *Periodica Polytechnica, Mechanical Engineering* 66 (2022): 325–335, https://doi.org/10.3311/PPme.20363.

13. X. Shi, M. K. Hassanzadeh-Aghdam, and R. Ansari, "Viscoelastic Analysis of Silica Nanoparticle-Polymer Nanocomposites," *Composites. Part B, Engineering* 158 (2019): 169–178, https://doi.org/10.1016/j.compositesb.2018.09.084.

14. R. J. Crawford and J. L. Throne, "6 - Processing," in *Plastics Design Library*, ed. R. J. Crawford and J. L. B. Throne (William Andrew Publishing, 2002), 201–306, https://doi.org/10.1016/B978-188420785-3.50008-3.

15. D. Rosato and D. Rosato, "2 - Design Optimization," in *BT - Plastics Engineered Product Design*, ed. D. Rosato and D. Rosato (Elsevier Science, 2003), 46–160, https://doi.org/10.1016/B978-185617416-9/50003-X.

16. A. Y. Malkin and A. I. Isayev, "2 - Viscoelasticity," in *Rheology Concepts, Methods, and Applications (Second Edition)*, ed. A. Y. Malkin and A. I. Isayev (Elsevier, 2012), 43–126, https://doi.org/10.1016/B978-1-895198-49-2.50007-4.

17. C. Gallegos and F. J. M. Boza, *Rheology* (Eolss, 2010).

18. S. Verma, B. Balasubramaniam, and R. K. Gupta, "Recycling, Reclamation and Re-Manufacturing of Carbon Fibres," *Current Opinion in Green and Sustainable Chemistry* 13 (2018): 86–90, https://doi.org/10.1016/j.cogsc.2018.05.011.

19. D. Chen, K. Molnar, H. Kim, et al., "Linear Viscoelastic Properties of Putative Cyclic Polymers Synthesized by Reversible Radical Recombination Polymerization (R3P)," *Macromolecules* 56 (2023): 1013–1032, https://doi.org/10.1021/acs.macromol.2c00892.

20. J. D. Ferry, *Viscoelastic Properties of Polymers* (Wiley, 1980), https://books.google.hu/books?id=9dqQY3Ujsx4C.

21. I. H. Syed, P. Vouagner, F. Fleck, and J. Lacayo-Pineda, "Nonlinearity in the Mechanical Response of Rubber as Investigated by High-Frequency DMA," *Polymers (Basel)* 11 (2019): E581, https://doi.org/10.3390/polym11040581.

22. M. Bek, J. Gonzalez-Gutierrez, C. Kukla, K. Pušnik Črešnar, B. Maroh, and L. Slemenik Perše, "Rheological Behaviour of Highly Filled Materials for Injection Moulding and Additive Manufacturing: Effect of Particle Material and Loading," *Applied Sciences* 10 (2020): 7993, https://doi.org/10.3390/app10227993.

23. I. Agirre-Olabide, M. J. Elejabarrieta, and M. M. Bou-Ali, "Matrix Dependence of the Linear Viscoelastic Region in Magnetorheological Elastomers," *Journal of Intelligent Material Systems and Structures* 26 (2015): 1880–1886, https://doi.org/10.1177/1045389X15580658.

24. N. Phewthongin, P. Sae-oui, and C. Sirisinha, "Rheological Behavior of Cpe/Nr Blends Filled With Precipitated Silica," *Journal of Applied Polymer Science* 100 (2006): 2565–2571, https://doi.org/10.1002/app.22550.

25. Z. Yang, S. Chaieb, Y. Hemar, L. de Campo, C. Rehm, and D. J. McGillivray, "Investigating Linear and Nonlinear Viscoelastic Behaviour and Microstructures of Gelatin-Multiwalled Carbon Nanotube

Composites," *RSC Advances* 5 (2015): 107916–107926, https://doi.org/10.1039/C5RA22744E.

26. R. Petrény, L. Almásy, and L. Mészáros, "Investigation of the Interphase Structure in Polyamide 6–Matrix, Multi-Scale Composites," *Composites Science and Technology* 225 (2022): 109489, https://doi.org/10.1016/j.compscitech.2022.109489.

27. O. Olejnik and A. Masek, "Bio-Based Packaging Materials Containing Substances Derived From Coffee and Tea Plants," *Materials (Basel)* 13 (2020): 5719, https://doi.org/10.3390/ma13245719.

28. P. Upadhyaya and S. Kumar, "Micromechanics of Stress Transfer Through the Interphase in Fiber-Reinforced Composites," *Mechanics of Materials* 89 (2015): 190–201, https://doi.org/10.1016/j.mechmat.2015.06.012.